

**FULL PAPER****Applied
Organometallic
Chemistry****WILEY**

***o*-Trityl phenoxy-imino vanadium (III) complexes: synthesis, characterization, and catalysis on ethylene (co) polymerization**

Zhiqiang Hao^{1,2} | Feng Li¹ | Wei Gao¹

¹College of Chemistry, Jilin University, Changchun, 130012, China

²Hebei Key Laboratory of Organic Functional Molecules, College of Chemistry & Material Science, Hebei Normal University, Shijiazhuang, 050024, China

Correspondence

Wei Gao, College of Chemistry, Jilin University, Changchun 130012, China.
Email: gw@jlu.edu.cn

Funding information

National Natural Science Foundation of China, Grant/Award Numbers: 21574052, 21603082, 51673078, U1462111

Several phenoxy-imine ligands bearing *o*-trityl group in phenoxy moiety $\text{RN}=\text{CHAROH}$ ($\text{Ar} = \text{C}_6\text{H}_2(\text{CPh}_3)^t\text{Bu}$, $R = 2,6\text{-Me}_2\text{C}_6\text{H}_3$ (**L₁H**); $2,6\text{-}^i\text{Pr}_2\text{C}_6\text{H}_3$ (**L₂H**); $3,5\text{-(CF}_3)_2\text{C}_6\text{H}_3$ (**L₃H**); $3,5\text{-(OMe)}_2\text{C}_6\text{H}_3$ (**L₄H**); CHPh_2 (**L₅H**); CPh_3 (**L₆H**)) were synthesized and characterized by ¹H NMR and ¹³C NMR spectroscopy. The vanadium complexes based on these ligands $\text{LVCl}_2(\text{THF})_2$ (**1–6**) were synthesized via conventional transmetalation reaction in moderate to high yields. Complexes **1–6** were fully characterized by FT-IR, elemental analyses and the molecular structures of **1**, **2**· H_2O , $(\text{2}\cdot\text{H}_2\text{O})_2(\mu\text{-Cl})_2$, **4**, and **5** were confirmed by X-ray crystallographic analysis in which the six-coordinated vanadium centers are in a typical octahedral geometry. Upon activation with Et_2AlCl in toluene, complexes **1–6** showed high activities in ethylene polymerization affording polymers with moderate molecular weight ($5.9\text{--}11.8 \times 10^4$ Da). Moreover, in hexane or CH_2Cl_2 , **1–6**/ Et_2AlCl exhibited enhanced activities. When activated with MAO or MMAO in toluene, these complexes showed relatively low activities but afforded polymers with ultra-high molecular weight (up to 3.30×10^6 Da). **1–6**/ Et_2AlCl also showed high activities in ethylene/1-hexene copolymerization at room temperature giving moderate molecular-weight polymers ($6.5\text{--}11.4 \times 10^4$ Da) with co-monomer incorporation being of $6.0 \sim 7.8\%$.

KEY WORDS

copolymerization, ethylene polymerization, ultra-high molecular weight, vanadium complexes

1 | INTRODUCTION

In the early 1960s, Ziegler-type vanadium catalyst systems, which were composed of vanadium complexes such as $\text{V}(\text{acac})_3$ and VOCl_3 , and organometallic reagents such as EtAlCl_2 and Et_2AlCl , were widely explored as homogeneous catalysts for olefin polymerization.^[1] These catalytic systems showed encouraging activities for synthesis of high molecular weight polymers with narrow polydispersity and good performance in co- and *ter*-polymerization of ethylene.^[1,2] Since then tremendous

efforts have been devoted in design and synthesis of new vanadium catalysts directed toward controlled polymerization. Various bidentate or polydentate ligands were incorporated to the systems and it is well accepted that the ancillary ligand which can render the metal centers tunable electronic or steric effects plays an important role in the catalytic performance.^[3–7] Of the numerous ligands used to support the vanadium complexes the phenoxy-imine (FI) derivatives, which have achieved great success in supporting group 4 complexes for olefin polymerization, have received great attention due to their

feasible tuning of electronic and steric effects by changing the groups in phenoxy and/or imine moiety.^[6f,8] For example, Fujita et al. have reported the bisligated vanadium (III) complexes with α phenoxy-imine ligands, which exhibited high activities in ethylene polymerization at 1 atm ethylene (**A** in chart 1).^[3b] Li and coworkers showed that the vanadium (III) complexes bearing FI ligands, upon activation with Et_2AlCl , exhibited high activities for ethylene polymerization giving polymers with moderate molecular weight.^[4a,f] Such catalytic system can also catalyze ethylene/1-hexene copolymerization producing polymers with low co-monomer incorporation and low molecular weights. Moreover, the vanadium complexes with FI ligands containing heteroatom exhibited slightly lower activities when compared to those with heteroatom-free ligands.^[4b] The vanadyl complexes bearing bidentate FI ligands, reported by Nomura, showed relatively lower activities affording polymers with broadened PDI.^[5e]

In the FI-based group 4 systems, it is well established that the *ortho* group in phenoxy moieties have a strong impact on the behaviors in olefin polymerizations.^[8] For example, the FI-Ti and FI-Zr complexes with *o*-tBu substituted ligands are usually more active than those with *o*-H substituted ligands respectively.^[8–10] Fujita disclosed that the FI-Ti catalysts bearing a cycloalkyl or *o*-phenyl group in *ortho* position produced high molecular-weight polymers with high catalyst efficiency and high α -olefin incorporation.^[11] DFT calculations revealed that the rotation of the *o*-phenyl group may evade the steric congestion during the polymerization.^[11] Despite extensive studies on the *ortho*-effects in FI group 4 systems, such effects in FI-Vanadium systems were less investigated and some limited reports gave inconsistent results. For example Nomura et al. demonstrated that, in the arylmido vanadium(V) complexes bearing FI ligands (**B** in chart 1), the size of *ortho* substitutes showed strong positive effects on the activities of ethylene polymerization.^[5e] Redshaw et al. demonstrated that the bridged mononuclear or dinuclear FI-V complexes with *o*-tBu group are more active than those without.^[6d]

Nevertheless, Li and co-workers reported that FI vanadium chlorides with *o*-tBu exhibited much lower catalytic activities when compared to those with *o*-H (**C** in chart 1). The author declared that the *o*-tBu group in the ligand may suppress the chain propagation during the polymerization.^[4a]

As part of our ongoing investigation in developing excellent vanadium catalysts for olefin polymerization, we are very interested in the vanadium complexes with *ortho* trityl FI ligands (see in chart 1). We envisioned that the rotation of the propeller-shape trityl moiety may furnish more efficient protection to the vanadium center. To this end, we herein report a series of *o*-trityl phenoxy-imine ligands (**L₁H–L₆H**) and their vanadium complexes. The catalytic performance of these complexes in ethylene polymerization and ethylene/1-hexene copolymerization are also presented.

2 | RESULTS AND DISCUSSION

2.1 | Synthesis and characterization of ligands L₁H–L₆H

The *ortho*-trityl FI ligands were synthesized according to the procedure described in Scheme 1. 4-*tert*-butyl-2-tritylphenol and 3-trityl-5-*tert*-butyl-salicylaldehyde were synthesized according to a procedure in the literature and identified by ¹H NMR and ¹³C NMR.^[12] Condensation reactions of 3-trityl-5-*tert*-butyl-salicylaldehyde with corresponding aniline afforded the 2-triphenylmethyl-4-*tert*-butylsalicylaldiminato derivatives (**L₁H – L₆H**) respectively in high yields (Scheme 1). The ligands were characterized by ¹H NMR and ¹³C NMR, in which the diagnostic resonances for the imino $\text{HC}=\text{NAr}$ were observed at 7.88–8.65 ppm. The sharp singlet at 12.63–13.94 ppm can be assigned to the OH group which linked to the imine nitrogen atoms via a hydrogen bond. The molecular structure of **L₆H** (Figure 1) established by X-ray diffraction analysis confirmed the coordinating potential of the ligand with the O atom and

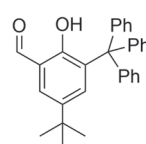
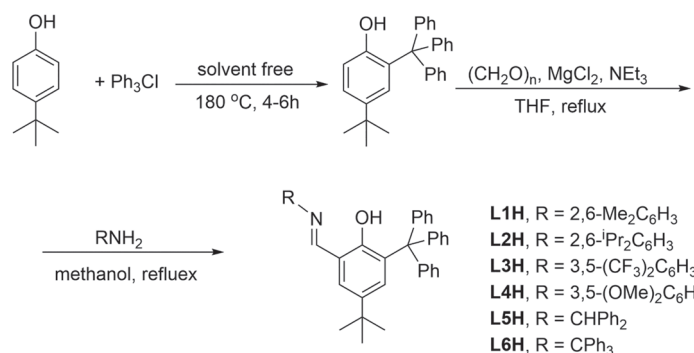
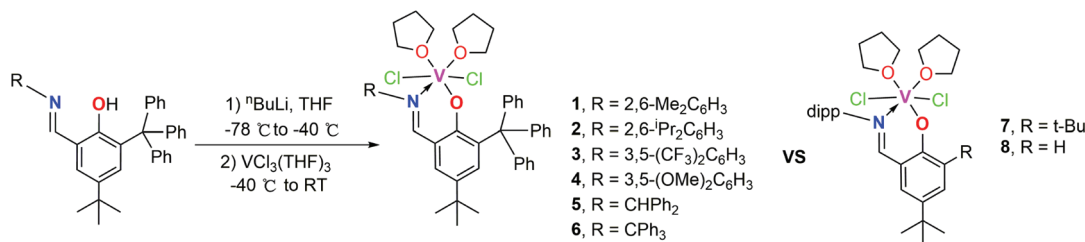
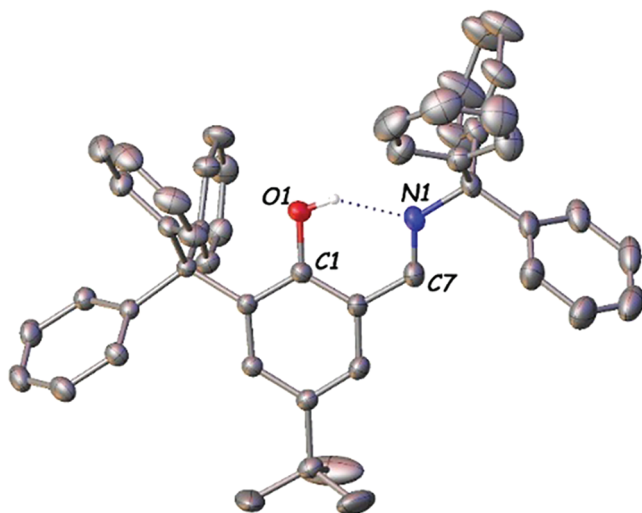


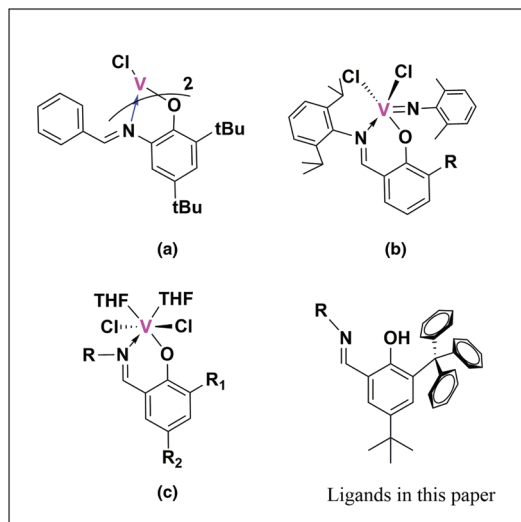
CHART 1 Typical FI vanadium complexes

**SCHEME 1** Synthetic routine for the ligands **L₁H-L₆H****FIGURE 1** Perspective view of **L₆H** with thermal ellipsoids drawn at 30% probability level. Hydrogens solvent are omitted for clarity. The selected bond lengths (Å): C(1)–O(1) 1.9630(18), C(7)–N(1) 2.066(2)

N atom linked by an intramolecular hydrogen bond. Two phenyl rings of the *o*-trityl group formed a V-shape shield surrounding the phenoxy group.

2.2 | Synthesis and characterization of vanadium complexes

The vanadium complexes (**1–6**) with the *ortho* trityl FI ligands were synthesized via a lithium-salt metathesis reaction (Scheme 2). Treatment of the ligands (**L₁H-L₆H**) with ⁿBuLi at -78 °C afforded corresponding ligand lithium salts as yellow solutions. After warm to -40 °C, 1 equiv of VCl₃(THF)₃ was added in one portion giving a red to brown solution. Evaporation of the solvent to dryness and crystallization of the residue with hexane/dichloromethane mixed solvent gave the vanadium complexes as dark red powders in moderate to high yields. Complexes **7** and **8** was also synthesized according to the literature for comparative studies.^[4a] Complexes **1–6** were characterized by FT-IR and elemental analyses.

**SCHEME 2** Synthesis of FI vanadium complexes **1–6** and the structures of complexes **7–8**

All the complexes showed broadened and informative resonances in ¹H{¹³C}NMR spectra indicating their paramagnetic nature. The efficient magnetic moments (μ_{eff}) of **1–6** determined by Evans method^[13] are in the range of 2.63–2.82 μ_{B} which are typical for a d^2 V (III) in high-spin state.^[4c,6d,14] The molecular structures of **1**, **2**·H₂O, **(2**·H₂O)₂(μ -Cl)₂**,** **4**, and **5** were further determined by X-ray crystallographic analysis and the summary of the crystal data and the structure determination results was listed in Table S1. Crystals of **1** suitable for X-ray crystallography were grown from THF/hexane mixed solution. The solid-state structure of **1** is shown in Figure 2 along with the selected bond lengths and angles in the caption. Complex **1** features a distorted octahedral geometry around the vanadium metal center which is coordinated by *o*-trityl FI ligand, two chlorine atoms, and two THF molecules. The bond distances of V1–O1 (1.919(6) Å) and V1–N1 (2.141(7) Å) are slightly longer than those respectively in [RN=CHARO]VCl₂(THF)₂ probably due to the repulsion of the trityl groups.^[4a] The two chlorine atoms and the two THF molecules in **1** are situated in *cis* position respectively as evidenced by the small Cl(1)–V(1)–

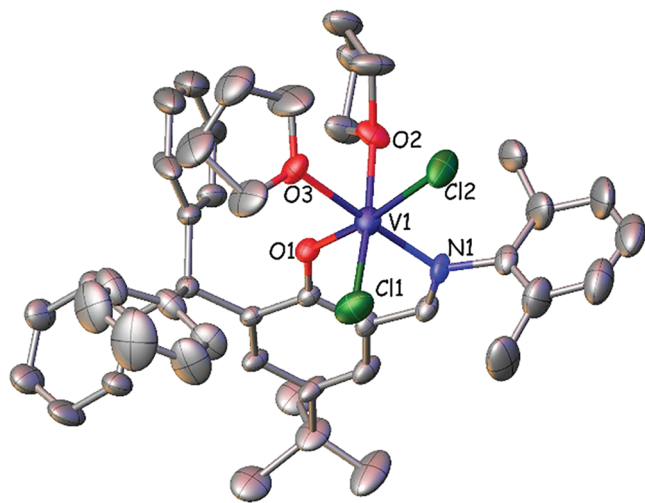


FIGURE 2 Perspective view of **1** with thermal ellipsoids drawn at 30% probability level. Hydrogens are omitted for clarity. The selected bond lengths (\AA) and angles (deg.): V(1)–O(1) 1.919(6), V(1)–O(2) 2.170(7), V(1)–O(3) 2.120(7), V(1)–N(1) 2.141(7), V(1)–Cl(1) 2.330(3), V(1)–Cl(2) 2.273(3); Cl(1)–V(1)–Cl(2) 95.57(15), N(1)–V(1)–O(1) 87.9(3), O(2)–V(1)–Cl(1) 174.7(2), O(2)–V(1)–O(3) 83.3(3), Cl(2)–V(1)–O(1) 169.8(2), O(3)–V(1)–N(1) 175.2(3)

Cl(2) angle ($87.9(3)^\circ$) and O(2)–V(1)–O(3) angle ($83.31(3)^\circ$). The vanadium atom is almost coplanar with the FI ligand plane with a deviation of (0.092 \AA). One of the THF molecules is situated in the valley formed by two aryl rings of *ortho*-trityl moiety. Such orientation can efficiently decrease the steric congestion at the metal

center. The aryl ring in imino moiety of **1** is almost perpendicular to the phenoxyl ring (dihedral angle of 91.75°). Attempts to grow the crystals of complex **2** in THF/hexane solution gave a hydrate complex **2**·H₂O (see in Figure 3), in which one of the THF molecule was replaced by a H₂O molecule from the solvent. The coordination of water molecule implies the good tolerance of the FI vanadium complexes to water. In **2**·H₂O the two chlorine atoms situate in *trans* position with the Cl(1)–V(1)–Cl(2) angle being of $170.90(5)^\circ$. The THF is in the *trans* position to the nitrogen atom in imine group. The metrical parameters of **2**·H₂O are very similar to those in **1**. It is worth to note that the vanadium atom deviates greatly from the FI coordination plane with a deviation of 0.269 \AA probably due to the repulsion of the isopropyl groups in the imine moiety. The crystals grown in dichloromethane solution of **2** gave out a THF-free dimeric complex $\{2\cdot\text{H}_2\text{O}\}_2(\mu\text{-Cl})$ in which two $[2,6\text{-}^i\text{Pr}_2\text{C}_6\text{H}_3\text{N}=\text{CHC}_6\text{H}_2(\text{CPh}_3)^i\text{Bu}]\text{V}(\text{H}_2\text{O})\text{Cl}$ units were connected by two chlorine bridges (see in Figure S1). The water molecule is in *trans* position to the terminal chlorine atom. The solid- structures of **4** and **5** were also confirmed by X-ray crystallography (Figures 4 and 5). In **4** the two chlorine atoms are in *trans* position whereas in **5** the two chlorine atoms are in *cis* position. The bond distances and angels in **4** and **5** are well comparable to those in **1**. The molecular structures described above reveal that, the incorporation of trityl group into the FI vanadium complexes may change the *cis/trans* configuration of the chlorine atoms (or THF molecules) probably due to the repulsion of the trityl

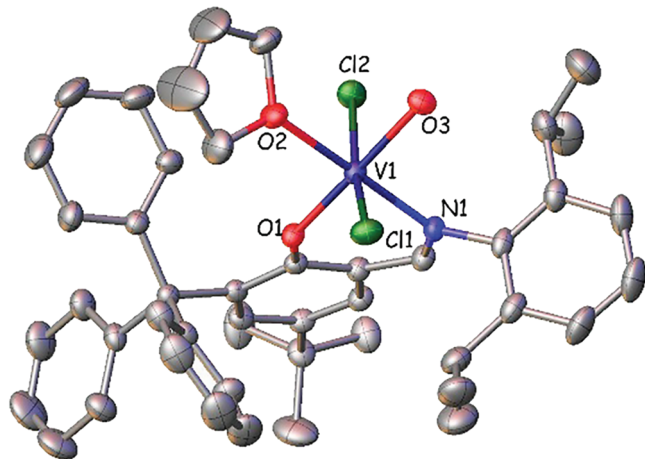


FIGURE 3 Perspective view of **2**·H₂O with thermal ellipsoids drawn at 30% probability level. Hydrogens are omitted for clarity. The selected bond lengths (\AA) and angles (deg.): V(1)–O(1) 1.8911(19), V(1)–N(1) 2.100(2), V(1)–O(2) 2.217(2), V(1)–O(3) 2.069(2), V(1)–Cl(1) 2.3793(8), V(1)–Cl(2) 2.3487(8); Cl(1)–V(1)–Cl(2) 168.60(3), O(1)–V(1)–O(3) 178.68(9), O(1)–V(1)–O(2) 91.07(8), N(1)–V(1)–O(1) 87.75(9)

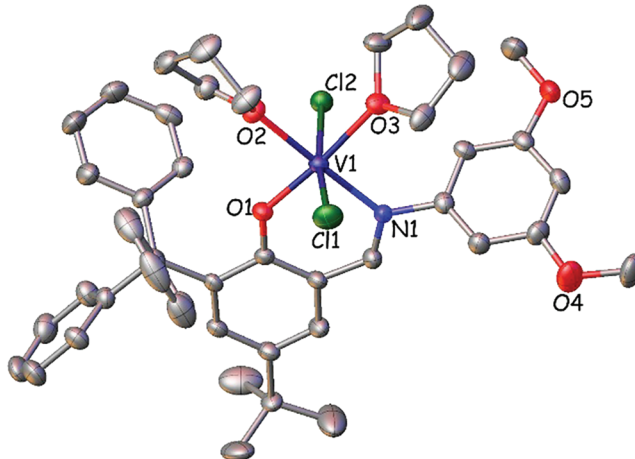


FIGURE 4 Perspective view of **4** with thermal ellipsoids drawn at 30% probability level. Hydrogens are omitted for clarity. The selected bond lengths (\AA) and angles (deg.): V(1)–O(1) 1.876(3), V(1)–N(1) 2.091(3), V(1)–O(2) 2.130(3), V(1)–O(3) 2.172(3), V(1)–Cl(1) 2.3297(12), V(1)–Cl(2) 2.3632(11); Cl(1)–V(1)–Cl(2) 170.90(5), O(1)–V(1)–N(1) 90.10(11), O(2)–V(1)–O(3) 84.52(10)

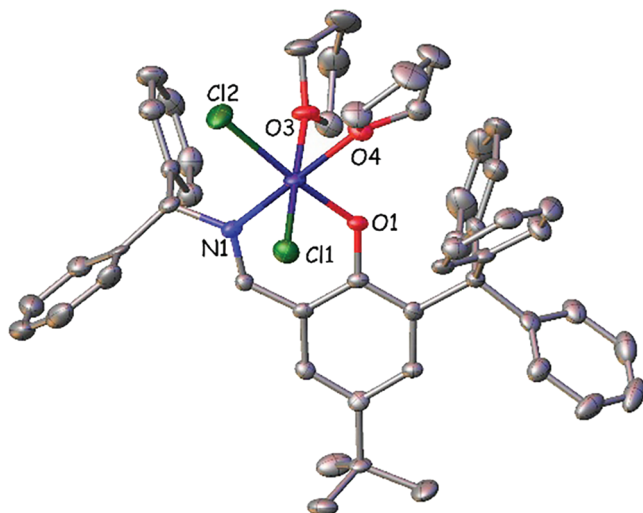


FIGURE 5 Perspective view of **5** with thermal ellipsoids drawn at 30% probability level. Hydrogens are omitted for clarity. The selected bond lengths (\AA) and angles (deg.): V(1)–O(1) 1.905(3), V(1)–N(1) 2.111(4), V(1)–O(2) 2.109(3), V(1)–O(3) 2.123(4), V(1)–Cl(1) 2.3326(15), V(1)–Cl(2) 2.3828(15); Cl(1)–V(1)–Cl(2) 92.50(6), O(1)–V(1)–N(1) 87.68(14)

group. But the bond lengths and angles involving metal center does not alter greatly when compared to the FI vanadium analogous with *o*-^tBu or *o*-H groups. The two phenyl rings stretch out to the outer sphere of the metal center. The out-sphere protection may not prohibit the uptake of monomer in the polymerization but may suppress the β -hydrogen elimination and chain transfer during the polymerization.

2.3 | Catalysis on olefin polymerization

Complexes **1–6** were evaluated as pre-catalysts for ethylene polymerization under the activation with Et₂AlCl. The polymerization results are listed in Table 1. The complexes [2,6-ⁱPr₂PhN=CH(C₆H₃^tBu₂O)VCl₂(THF)₂] (**7**) and [2,6-ⁱPr₂PhN=CH(C₆H₃^tBu)O]VCl₂(THF)₂ (**8**) were also tested for comparation. Complexes **1–6** showed low activity for ethylene polymerization when only Et₂AlCl was used. As proven previously, the poor activity may be ascribed to the reduction of the V (III) to low valent species during the activation with alkyl aluminum compounds.^[2g] Some oxidant reagent such as Cl₃CCO₂Et were generally needed to maintain the activity. As expected, when small amount of Cl₃CCO₂Et was added the **1–6**/Et₂AlCl catalytic systems showed high activities in ethylene polymerization. For example, the productivity of 4.28×10^4 Kg PE·mol (V)⁻¹·h⁻¹ was obtained by using 0.1 μ mol of **1** and 1,000 equiv of Et₂AlCl at room temperature in the presence of 0.03 mL Cl₃CCO₂Et. The activity

showed slight dependence on the Al/V ratio and the activity of **1** increased from 4.28×10^4 to 5.08×10^4 Kg PE·mol (V)⁻¹·h⁻¹ when Al/V ratio increased from 1,000:1 to 2000:1. But further increase the Al/V ratio to 3,000:1 the activity drops slightly. Interestingly, the molecular weights of the polymer were not affected greatly by the Al/V ratio in the range of 1,000 ~ 3,000 (entry 1–3). It was reported that, in the catalytic systems with **7** or **8**, the molecular weight of the polymer decreased gradually with the increase of Et₂AlCl concentration probably due to the chain transfer from vanadium to aluminum.^[4a] We believe that in the *o*-trityl FI-vanadium systems the chain migration from the active species to the aluminum species may be suppressed by the bulky *ortho*-^tPr group. The polymerization temperature showed little influence on the activities. The catalytic activities of complex **1** decrease slightly with an increase of temperature, while the molecular weights of the resulted polymers are not varied greatly with temperature. Upon activation with 2000 equiv of Et₂AlCl at room temperature complexes **2–6** also showed high activities in ethylene polymerization. Complex **2** with two bulky *ortho*-ⁱPr groups in the N-aryl moiety showed higher activities than **1** under the same condition (entry 6). On introducing two trifluoromethyl (electron-withdrawing group) into the 3,5-positions of N-aryl moiety, to form complex **3**, catalytic activity did not change much when compared with the system involving **1**. However, when two methoxyl (donating group) were introduced into the 3,5-position of N-aryl moiety in the ligand the activity decreased about 20%. Complex **5** which possess a cumyl group in imino moiety showed the highest activity among these complexes. Further increase the steric hindrance around the metal center by introducing a Ph₃C group in imino moiety, to form complex **6**, the activity decreases slightly. The decrease in activity should be ascribed to that the bulky substitutes may suppress the chain propagation during the polymerization. A great deal of research has shown that solvent play an important role in vanadium system for olefin polymerization. For example, the ethylene polymerization with VCl₂(N-2,6-Me₂C₆H₃)(O-Me₂C₆H₃)/Et₂AlCl in CH₂Cl₂ exhibited higher activities than in toluene, while the activities in n-hexane were very low.^[5g] Our catalytic systems of **1–6**/Et₂AlCl showed enhanced activities in CH₂Cl₂ affording the polymers with high molecular weight (entry 11 ~ 16) in which complex **4** showed the highest activities and the productivity up to 7.52×10^4 Kg PE·mol (V)⁻¹·h⁻¹ was obtained. Unexpectedly, **1–6**/Et₂AlCl showed very high activity in hexane (entry 17 ~ 22) and a productivity of 6.72×10^4 Kg PE·mol (V)⁻¹·h⁻¹ was obtained with **3**/Et₂AlCl/in hexane. This result is in contrast to the VCl₂(N-2,6-Me₂C₆H₃)(O-Me₂C₆H₃)/Et₂AlCl system which showed

TABLE 1 Polymerization of ethylene with **1–6/Et₂AlCl**^a

Entry	Catalyst	Al/V	T (°C)	Solvent	Yield (g)	Activity ^b ($\times 10^4$)	M_w^c ($\times 10^4$)	PDI	M.p. ^d
1	1	1,000	25	Toluene	1.07	4.28	8.4	2.5	138.3
2	1	2000	25	Toluene	1.27	5.08	9.1	2.6	139.5
3	1	3,000	25	Toluene	1.14	4.56	9.7	2.9	139.7
4	1	2000	50	Toluene	1.12	4.48	10.2	2.9	138.8
5	1	2000	70	Toluene	1.08	4.32	9.0	2.8	139.4
6	2	2000	25	Toluene	1.35	5.40	6.4	2.4	137.6
7	3	2000	25	Toluene	1.23	4.92	11.8	1.8	141.4
8	4	2000	25	Toluene	1.02	4.08	11.1	2.7	141.1
9	5	2000	25	Toluene	1.44	5.76	9.9	2.8	139.5
10	6	2000	25	Toluene	1.14	4.56	8.3	2.2	141.3
11	1	2000	25	CH ₂ Cl ₂	1.39	5.56	8.2	2.6	140.3
12	2	2000	25	CH ₂ Cl ₂	1.60	6.40	6.5	2.7	139.7
13	3	2000	25	CH ₂ Cl ₂	1.85	7.40	11.6	2.9	138.4
14	4	2000	25	CH ₂ Cl ₂	1.88	7.52	7.3	3.1	139.3
15	5	2000	25	CH ₂ Cl ₂	1.40	5.60	6.4	2.7	142.9
16	6	2000	25	CH ₂ Cl ₂	1.15	4.60	5.9	2.8	137.9
17	1	2000	25	Hexane	1.48	5.92	6.1	2.7	142.2
18	2	2000	25	Hexane	1.61	6.44	7.3	2.6	141.0
19	3	2000	25	Hexane	1.68	6.72	8.8	2.4	139.9
20	4	2000	25	Hexane	1.66	6.64	8.6	2.5	139.2
21	5	2000	25	Hexane	1.53	6.12	7.4	2.8	139.6
22	6	2000	25	Hexane	1.25	5.00	7.8	2.7	140.1
23	VCl ₃ (THF) ₃	2000	25	Toluene	0.88	3.22	18.2	5.6	140.2
24	7	2000	25	Toluene	1.04	4.08	5.2	2.8	139.8
25	8	2000	25	Toluene	1.52	6.41	4.3	2.4	139.9

^aPolymerization conditions: solvent (60 ml), cat (0.1 μ mol based on V), Cl₃CCO₂Et = 0.03 mL; 5 bar; 15 min.

^bActivity in unit of Kg PE·mol(V)⁻¹·h⁻¹.

^cDetermined by GPC relative to polystyrene standards.

^dDetermined by DSC at a heating of 10 °C min⁻¹.

very low activity in hexane.^[5g] Complexes **7** and **8** with small *ortho* group in ligand showed similar activities under the same conditions affording the polymers with relative lower molecular-weight when compared with those derived from *o*-trityl FI vanadium systems. This result suggested that the bulky *o*-trityl group which offer an efficient out-sphere protection may suppress the chain-transfer and β -H elimination during the polymerization giving the polymers with relatively high molecular-weight. The ¹³C NMR spectroscopy analysis shows that all the polymers obtained with **1–6/Et₂AlCl** catalytic systems are highly linear with the melting point in the range of 137.6–142.9 °C (see Figure S2).

When MAO or MMAO was used as co-catalyst, complexes **1–6** show relatively lower activities compared to

those with Et₂AlCl (Table 2). Interestingly, the molecular weights of the resulted polymer derived from the **1–6/MAO** (MMAO) are greatly higher than those with Et₂AlCl and the polymers with molecular weight up to 3.30×10^6 Da were obtained with **2/MMAO** at room temperature (see Figure S4).

Complexes **1–6** were also used to catalyze the ethylene/hexene copolymerization and the representative results are summarized in Table 3. When activated with Et₂AlCl, complexes **1–6** show high activities toward ethylene/hexene copolymerization and give the high molecular weight copolymers with unimodal molecular weight distributions (D 2.8 ~ 3.6). The co-monomer incorporations of 6.0 ~ 7.8% were obtained. The representative ¹³C NMR and GPC data of the polymer see Figure S3 and S5.

TABLE 2 Polymerization of ethylene with 1–6/MAO (MMAO)^a

Entry	Catalyst	Co-catalyst	Yield (g)	Activity ^b	Mw ^c ($\times 10^6$)	PDI	M.p. ^d
1	1	MAO	0.12	960	1.68	1.9	135.5
2	2	MAO	0.28	2,240	1.75	2.1	138.1
3	3	MAO	0.15	1,200	1.13	1.6	138.4
4	4	MAO	0.27	2,160	0.87	2.7	136.4
5	5	MAO	0.34	2,720	1.35	2.6	136.8
6	6	MAO	0.16	1,280	1.27	2.3	137.1
7	1	MMAO	0.28	2,240	2.64	1.7	137.1
8	2	MMAO	0.49	3,920	3.30	2.5	138.0
9	3	MMAO	0.36	2,880	2.68	2.4	135.5
10	4	MMAO	0.30	2,400	2.69	2.4	135.7
11	5	MMAO	0.58	4,640	2.89	2.3	136.2
12	6	MMAO	0.23	1840	2.26	2.0	136.7

^aPolymerization conditions: toluene (60 ml), cat (0.5 μ mol based on V), $\text{Cl}_3\text{CCO}_2\text{Et}$ = 0.05 ml, Al/V molar ratio = 400, temperature 25 °C, ethylene pressure 5 bar, time 15 min.

^bActivity in unit of Kg of PE·mol (V)⁻¹·h⁻¹.

^cDetermined by GPC relative to polystyrene standards.

^dDetermined by DSC at a heating of 10 °C min⁻¹.

TABLE 3 Ethylene/1-hexene copolymerization **1–6/Et₂AlCl**^a

Run	Catalyst	Al/V	Yield (g)	Activity ^b ($\times 10^3$)	Hexene ^c content	Mw ^d ($\times 10^4$)	PDI
1	1	400	1.79	7.2	7.1	8.5	3.0
2	2	400	1.65	6.5	6.0	8.9	3.4
3	3	400	2.55	10.2	7.8	5.6	2.9
4	4	400	2.85	11.4	7.0	5.1	2.8
5	5	400	1.70	6.8	6.6	11.1	3.6
6	6	400	1.69	6.7	6.9	11.5	3.5

^aPolymerization conditions: toluene 60 ml, 1.0 μ mol, $\text{Cl}_3\text{CCO}_2\text{Et}$ = 0.05 ml, 15 min, hexene 0.75 mol/l, temperature 25 °C.

^bActivity in unit of Kg of PE·mol (V)⁻¹·h⁻¹.

^cCalculated on the basis of ¹³C NMR spectra.

^dDetermined by GPC relative to polystyrene standards.

3 | CONCLUSION

A series of o-trityl phenoxy-imine ligands were synthesized and used to support the vanadium (III) complexes. All these complexes were fully characterized and some of their solid structures were further confirmed by X-ray diffraction analysis in which the vanadium atoms are in distorted octahedral geometry. When combined with Et₂AlCl, these complexes showed high activities for ethylene polymerization (activities up to 7.52×10^4 g·mol⁻¹(V)·h⁻¹) affording the polymers with moderate molecular-weight. While MAO (MMAO) was used, these complexes can polymerize ethylene to ultra-high molecular weight polymers (up to 3.30×10^6 Da) with narrow PDI (<3). These complexes also showed high activities in the copolymerization of ethylene with

1-hexene affording the polymers with moderate comonomer incorporations (6.0 ~ 7.8%).

4 | EXPERIMENTAL

4.1 | General considerations

All manipulations involving air- and moisture-sensitive compounds were carried out under an atmosphere of dried and purified nitrogen using standard Schlenk and vacuum-line techniques. Toluene and THF were dried over sodium metal and distilled under nitrogen prior to use. Elemental analyses were performed on a Varian EL microanalyzer. CH₂Cl₂, hexane and 1-hexene were purified by distilling over calcium hydride before use. NMR

spectra were carried out on a Varian 400 MHz instrument at room temperature in CDCl_3 solution for ligands. ^{13}C NMR spectra of the copolymers were recorded on a Varian Unity-400 NMR spectrometer at 135 °C with *o*- $\text{C}_6\text{D}_4\text{Cl}_2$ as the solvent. The molecular weights (MWs) and polydispersity indices (PDIs) of the polymer samples were determined at 150 °C by a PL-GPC 220 type high-temperature gel permeation chromatograph. 1,2,4-Trichlorobenzene was employed as the solvent at a flow rate of 1.0 mL/min. The differential scanning calorimetry (DSC) measurements were performed on a Netzsch DSC 204 instrument under a N_2 atmosphere. The samples were heated at a rate of 10 °C/min and cooled at a rate of 10 °C/min. The melting peaks were obtained by analyzing the second heating graph. 3,5-Bis (trifluoromethyl)aniline, 3,5-dimethoxyaniline, triphenylmethanamine, diphenylmethanamine, and triphenylchloromethane were purchased from Aldrich. Ethyl trichloroacetate (ETA) was purchased from TCI. 5-*tert*-butyl-2-hydroxy-3-tritylbenzaldehyde^[12] and $\text{VCl}_3(\text{THF})_3$ was prepared according to the literature.^[15] The representative ^{13}C NMR and GPC data of the polymers are given in Figures S2-S5.

4.2 | Synthesis of ligands L_1H - L_6H

4.2.1 | Synthesis of L_1H

5-*tert*-butyl-2-hydroxy-3-tritylbenzaldehyde (2.10 g, 5.00 mmol) and 2,6-dimethylaniline (0.91 g, 7.50 mmol) was dissolved in 30 ml of anhydrous methanol, and a few drops of formic acid were added. After refluxing for 12 hr the mixture was evaporated to dryness and the residue was treated with cold methanol to give the L_1H as yellow powder. Yield 2.27 g (86.7%). ^1H NMR (400 MHz, CDCl_3 , 25 °C): δ 1.20 (t, 9H, C (CH_3)₃), 2.08 (s, 6H, Ar-CH₃), 6.92–6.96 (t, 1H, Ar-H), 7.01–7.03 (d, 2H, Ar-H), 7.14–7.18 (t, 4H, Ar-H), 7.22–7.29 (m, 12H, Ar-H), 7.45 (s, 1H, Ar-H), 8.29 (s, 1H, CH=N), 13.19 (s, 1H, Ar-OH) ppm. ^{13}C NMR (100 MHz, CDCl_3 , 25 °C): δ 18.47 (s, 2C, Ar-CH₃), 31.38 (s, 3C, C (CH_3)₃), 34.20 (s, 1C, C (CH_3)₃), 63.52 (s, 1C, C (Ph)₃), 118.06, 124.70, 125.62, 127.18, 127.47, 127.68, 128.23, 128.31, 131.10, 132.69, 134.58, 140.17, 145.60, 148.03, 158.18, 166.95 (s, 1C, CH=N) ppm.

4.2.2 | Synthesis of L_2H

L_2H was synthesized in the same way as described for L_1H using 5-*tert*-butyl-2-hydroxybenzaldehyde (2.10 g, 5.00 mmol) and 2,6-diisopropylaniline (1.33 g,

7.50 mmol). L_2H was obtained as yellow solid. Yield 2.56 g (88.3%). ^1H NMR (400 MHz, CDCl_3 , 25 °C): δ 1.07–1.09 (d, 12H, CH (CH_3)₂), 1.21 (s, 9H, C (CH_3)₃), 2.81–2.88 (m, 2H, CH (CH_3)₂), 7.10 (s, 2H, Ar-H), 7.15–7.18 (t, 3H, Ar-H), 7.22–7.30 (m, 14H, Ar-H), 7.46 (s, 1H, Ar-H), 8.24 (s, 1H, CH=N), 13.30 (s, 1H, Ar-OH) ppm. ^{13}C NMR (100 MHz, CDCl_3 , 25 °C): δ 23.45 (s, 4C, ArCH (CH_3)₂), 28.06 (s, 2C, ArCH (CH_3)₂), 31.36 (s, 3C, C (CH_3)₃), 34.20 (s, 1C, C (CH_3)₃), 63.53 (s, 1C, C (Ph)₃), 117.95, 123.11, 125.19, 125.61, 127.16, 127.39, 131.08, 132.75, 134.69, 138.65, 140.18, 145.58, 146.10, 158.23, 166.68 (s, 1C, CH=N) ppm.

4.2.3 | Synthesis of L_3H

L_3H was synthesized in the same way as described for L_1H using 5-*tert*-butyl-2-hydroxybenzaldehyde (2.10 g, 5.00 mmol) and 3,5-bis (trifluoromethyl)aniline (1.72 g, 7.50 mmol). L_3H was obtained as yellow solid. Yield 2.67 g (84.5%). ^1H NMR (400 MHz, CDCl_3 , 25 °C): δ 1.22 (s, 9H, C (CH_3)₃), 7.18–7.25 (m, 15H, Ar-H), 7.37 (s, 1H, Ar-H), 7.52 (s, 1H, Ar-H), 7.60 (s, 2H, Ar-H), 7.72 (s, 1H, Ar-H), 8.65 (s, 1H, CH=N), 12.63 (s, 1H, Ar-OH) ppm. ^{13}C NMR (100 MHz, CDCl_3 , 25 °C): δ 31.25 (s, 3C, C (CH_3)₃), 34.26 (s, 1C, C (CH_3)₃), 63.70 (s, 1C, C (Ph)₃), 118.07, 119.72, 121.56, 121.71, 124.42, 125.74, 127.26, 128.47, 130.99, 132.62, 132.95, 134.01, 134.79, 141.03, 145.25, 149.98, 158.16, 165.88 (s, 1C, CH=N) ppm.

4.2.4 | Synthesis of L_4H

L_4H was synthesized in the same way as described for L_1H using 5-*tert*-butyl-2-hydroxybenzaldehyde (2.10 g, 5.00 mmol) and 3,5-dimethoxyaniline (1.15 g, 7.50 mmol). L_4H was obtained as yellow solid. Yield 2.21 g (79.7%). ^1H NMR (400 MHz, CDCl_3 , 25 °C): δ 1.20 (s, 9H, C (CH_3)₃), 3.77 (s, 6H, Ar-OCH₃), 6.35–6.39 (m, 3H, Ar-H), 7.18–7.31 (m, 16H, Ar-H), 7.42 (s, 1H, Ar-H), 8.59 (s, 1H, CH=N), 13.23 (s, 1H, Ar-OH) ppm. ^{13}C NMR (100 MHz, CDCl_3 , 25 °C): δ 31.30 (s, 3C, C (CH_3)₃), 34.15 (s, 1C, C (CH_3)₃), 55.53 (s, 2C, Ar-OCH₃), 63.43 (s, 1C, C (Ph)₃), 99.17, 99.38, 118.42, 125.63, 127.19, 127.89, 131.03, 132.76, 134.35, 140.34, 145.48, 150.39, 157.99, 161.26, 163.16 (s, 1C, CH=N) ppm.

4.2.5 | Synthesis of L_5H

L_5H was synthesized in the same way as described for L_1H using 5-*tert*-butyl-2-hydroxybenzaldehyde (2.10 g, 5.00 mmol) and aminodiphenylmethane (1.37 g, 7.50 mmol). L_5H was obtained as yellow solid. Yield

2.38 g (81.4%). ^1H NMR (400 MHz, CDCl_3 , 25 °C): δ 1.15 (s, 9H, C (CH_3)₃), 5.54 (s, 1H, CH (Ph)₂), 7.15–7.20 (m, 12H, Ar-H), 7.22–7.27 (m, 14H, Ar-H), 7.35 (s, 1H, Ar-H), 8.40 (s, 1H, CH=N), 13.30 (s, 1H, Ar-OH) ppm. ^{13}C NMR (100 MHz, CDCl_3 , 25 °C): δ 31.38 (s, 3C, C (CH_3)₃), 34.14 (s, 1C, C (CH_3)₃), 63.53 (s, 1C, C (Ph)₃), 76.72 (s, 1C, N-CH (Ph)₂) 125.57, 118.29, 127.17, 127.27, 127.38, 127.69, 128.55, 131.10, 132.04, 134.20, 139.98, 142.44, 145.64, 157.81, 165.61 (s, 1C, CH=N) ppm.

4.2.6 | Synthesis of $\mathbf{L}_6\mathbf{H}$

$\mathbf{L}_6\mathbf{H}$ was synthesized in the same way as described for $\mathbf{L}_1\mathbf{H}$ using 5-*tert*-butyl-2-hydroxybenzaldehyde (2.10 g, 5.00 mmol) and tritylamine (1.30 g, 7.50 mmol). $\mathbf{L}_6\mathbf{H}$ was obtained as yellow solid. Yield 2.83 g (85.6%). ^1H NMR (400 MHz, CDCl_3 , 25 °C): δ 1.13 (s, 9H, C (CH_3)₃), 6.97 (s, 1H, Ar-H), 7.08–7.10 (m, 6H, Ar-H), 7.14–7.18 (m, 3H, Ar-H), 7.21–7.29 (m, 21H, Ar-H), 7.37 (s, 1H, Ar-H), 7.88 (s, 1H, CH=N), 13.94 (s, 1H, Ar-OH) ppm. ^{13}C NMR (100 MHz, CDCl_3 , 25 °C): δ 31.52 (s, 3C, C (CH_3)₃), 34.26 (s, 1C, C (CH_3)₃), 63.70 (s, 1C, C (Ph)₃), 78.83 (s, 1C, N-C (Ph)₃) 118.34, 125.66, 127.27, 127.89, 128.07, 129.84, 131.28, 132.19, 134.52, 139.96, 144.42, 145.82, 158.26, 164.56 (s, 1C, CH=N) ppm.

4.3 | Synthesis of vanadium complexes 1–6

4.3.1 | Synthesis of complex 1

$^n\text{BuLi}$ (0.5 mL, 1.00 mmol) in n-hexane was added dropwise to a stirred solution of $\mathbf{L}_1\mathbf{H}$ (0.52 g, 1.00 mmol) in 30 ml of THF at –78 °C. The mixture was allowed to warm to –40 °C and stirred for 30 min. $\text{VCl}_3(\text{THF})_3$ (0.38 g, 1.00 mmol) was added in one portion and the mixture was allowed to warm to room temperature and stirred overnight. After removal of the solvent, the residue was extracted with toluene (20 ml). Toluene was removed in vacuum and the crude product was recrystallized from CH_2Cl_2 /hexane to give the pure complex **1** as dark red powder (0.52 g, 65.7%). Anal. Calcd for $\text{C}_{46}\text{H}_{52}\text{Cl}_2\text{NO}_3\text{V}(\%)$: C, 70.05; H, 6.64; N, 1.78. Found: C, 70.21; H, 6.49; N, 1.64. $\mu_{\text{eff}} = 2.81\mu_{\text{B}}$. IR (KBr): ν (cm^{–1}) 3020w, 2,935 m, 2,864 m, 1,603 m, 1504vs, 1421s, 867 m, 820 s, 682w, 601 m, 512w.

4.3.2 | Synthesis of complex 2

Complex **2** was synthesized in the same way as described above for complex **1** using $\mathbf{L}_2\mathbf{H}$ (0.58 g, 1.00 mmol),

$^n\text{BuLi}$ (2.00 M in hexane, 0.50 ml, 1.00 mmol), and $\text{VCl}_3(\text{THF})_3$ (0.38 g, 1.00 mmol). Complex **2** was obtained as dark red powders (yield 0.53 g, 62.5%). The crystals of **2** suitable for X-ray structural determination were grown from THF/hexane mixed solution. Anal. Calcd for $\text{C}_{50}\text{H}_{60}\text{Cl}_2\text{NO}_3\text{V}(\%)$: C, 71.08; H, 7.16; N, 1.66. Found: C, 70.92; H, 7.03; N, 1.79. $\mu_{\text{eff}} = 2.78\mu_{\text{B}}$. IR (KBr): ν (cm^{–1}) 3016w, 2,920 m, 2861w, 1,605 m, 1494vs, 1,445 m, 1389s, 870w, 821 s, 676w, 599 m.

4.3.3 | Synthesis of complex 3

Complex **3** was synthesized in the same way as described above for complex **1** using $\mathbf{L}_3\mathbf{H}$ (0.63 g, 1.00 mmol), $^n\text{BuLi}$ (2.00 M in hexane, 0.50 mL, 1.00 mmol), and $\text{VCl}_3(\text{THF})_3$ (0.38 g, 1.00 mmol). Complex **3** was obtained as dark red powders (yield 0.53 g, 58.8%). Anal. Calcd for $\text{C}_{46}\text{H}_{46}\text{Cl}_2\text{F}_6\text{NO}_3\text{V}(\%)$: C, 61.61; H, 5.17; N, 1.56. Found: C, 61.80; H, 5.28; N, 1.41. $\mu_{\text{eff}} = 2.63\mu_{\text{B}}$. IR (KBr): ν (cm^{–1}) 3014w, 2,927 m, 2,868 m, 1,607 m, 1487vs, 1,453 m, 1,392 m, 877w, 824 s, 690w, 606 m, 503w.

4.3.4 | Synthesis of complex 4

Complex **4** was synthesized in the same way as described above for complex **1** using $\mathbf{L}_4\mathbf{H}$ (0.56 g, 1.00 mmol), $^n\text{BuLi}$ (2.00 M in hexane, 0.50 mL, 1.00 mmol), and $\text{VCl}_3(\text{THF})_3$ (0.38 g, 1.00 mmol). Complex **4** was obtained as dark red powders (yield 0.55 g, 66.8%). The crystals of **4** suitable for X-ray structural determination were grown from THF/hexane mixed solution. Anal. Calcd for $\text{C}_{46}\text{H}_{52}\text{Cl}_2\text{NO}_5\text{V}(\%)$: C, 67.32; H, 6.39; N, 1.71. Found: C, 67.19; H, 6.27; N, 1.86. $\mu_{\text{eff}} = 2.77\mu_{\text{B}}$. IR (KBr): ν (cm^{–1}) 2958 s, 2840 m, 2715w, 1730vs, 1584w, 1467s, 1,377 m, 1155s, 1071w, 981 m, 836 m, 739w, 496w.

4.3.5 | Synthesis of complex 5

Complex **5** was synthesized in the same way as described above for complex **1** using $\mathbf{L}_5\mathbf{H}$ (0.58 g, 1.00 mmol), $^n\text{BuLi}$ (2.00 M in hexane, 0.50 ml, 1.00 mmol), and $\text{VCl}_3(\text{THF})_3$ (0.38 g, 1.00 mmol). Complex **5** was obtained as dark red powders (yield 0.61 g, 71.2%). The crystals of **5** suitable for X-ray structural determination were grown from THF/hexane mixed solution. Anal. Calcd for $\text{C}_{51}\text{H}_{54}\text{Cl}_2\text{NO}_3\text{V}(\%)$: C, 71.99; H, 6.40; N, 1.65. Found: C, 72.16; H, 6.58; N, 1.45. $\mu_{\text{eff}} = 2.82\mu_{\text{B}}$. IR (KBr): ν (cm^{–1}) 3027w, 2,952 m, 2854w, 1619s, 1536w, 1,487 m, 1,439 m, 1314w, 1,002 m, 843w, 752 m, 697vs, 551 m.

4.3.6 | Synthesis of complex 6

Complex **6** was synthesized in the same way as described above for complex **5** using **L₆H** (0.66 g, 1.00 mmol), ⁿBuLi (2.00 M in hexane, 0.50 ml, 1.00 mmol), and VCl₃(THF)₃ (0.38 g, 1.00 mmol). Complex **6** was obtained as dark red powders (yield 0.69 g, 74.3%). Anal. Calcd for C₅₇H₅₈Cl₂NO₃V(%): C, 73.86; H, 6.31; N, 1.51. Found: C, 73.69; H, 6.47; N, 1.69. $\mu_{\text{eff}} = 2.79 \mu_{\text{B}}$. IR (KBr): ν (cm⁻¹) 3008w, 2,930 m, 2,867 m, 1,612 m, 1495vs, 1,446 m, 1397s, 868 m, 822 s, 683w, 600 m, 509w.

4.4 | Ethylene polymerization experiments

The ethylene polymerization experiments were carried out as follows: a dry 100 mL steel autoclave with a magnetic stirrer was charged with 55 ml of toluene, thermostated at the desired temperature, and saturated with ethylene (1.0 atm). The polymerization reaction was started by addition of a mixture of the catalyst and co-catalyst in toluene (5 ml) at the same time. The vessel was pressurized to 5 atm with ethylene immediately, and the pressure was maintained by continuous feeding of ethylene. The mixture was stirred at the desired temperature for the desired time period. The polymerization was then quenched by injecting an acidic ethanol solution containing HCl (3 M). The polymer was collected by filtration, washed with water and ethanol, and dried to a constant weight under vacuum.

4.5 | Crystallography

The crystals were mounted on a glass fiber using the oil drop. Data obtained with the ω -2 θ scan mode were collected on a Bruker SMART 1000 CCD diffractometer with graphite-monochromated $K\alpha$ radiation ($\lambda = 0.71073 \text{ \AA}$). The structures were solved using direct methods, while further refinement with full-matrix least squares on F^2 was obtained with the SHELXTL program package. All non-hydrogen atoms were refined anisotropically. Hydrogen atoms were introduced in calculated positions with the displacement factors of the host carbon atoms. The crystal data and summary of X-ray data collection are given in Table S1 in Supporting Information.

ACKNOWLEDGMENTS

We thank financial supports from the National Natural Science Foundation of China for project Nos. 21574052, U1462111, 51673078, 21603082.

ORCID

Zhiqiang Hao  <https://orcid.org/0000-0002-6554-803X>

REFERENCES

- [1] a) W. L. Carrick, *J. Am. Chem. Soc.* **1958**, *80*, 6455; b) W. L. Carrick, R. W. Kluiber, E. F. Bonner, L. H. Wartman, F. M. Rugg, J. Smyth, *J. Am. Chem. Soc.* **1960**, *82*, 3883; c) G. Natta, G. Mazzanti, A. Valvassori, G. Sartori, D. Fiumani, *J. Polym. Sci. A* **1961**, *51*, 411; d) G. W. Phillips, W. L. Carrick, *J. Polym. Sci. A* **1962**, *59*, 401; e) V. E. Junghanns, A. Gumboldt, G. Bier, *Makromol. Chem.* **1962**, *58*, 18; f) D. L. Christman, G. I. Keim, *Macromolecules* **1968**, *1*, 358.
- [2] a) Y. Doi, S. Ueki, T. Keii, *Macromolecules* **1979**, *12*, 814; b) Y. Doi, T. Koyama, K. Soga, *Makromol. Chem.* **1985**, *186*, 11; c) H. Hagen, J. Boersma, G. van Koten, *Chem. Soc. Rev.* **2002**, *31*, 357; d) S. Gambarotta, *Coord. Chem. Rev.* **2003**, *237*, 229; e) K. Nomura, W. Zhang, *Chem. Sci.* **2010**, *1*, 161; f) C. Redshaw, *Dalton Trans.* **2010**, *39*, 5595. K. Nomura, S. Zhang, *Chem. Rev.* **2010**, *111*, 2342; g) G. Zanchin, L. Vendier, I. Pierro, F. Bertini, G. Ricci, C. Lorber, G. Leone, *Organometallics* **2018**, *37*, 3181.
- [3] a) Y. Nakayama, H. Bando, Y. Sonobe, Y. Suzuki, T. Fujita, *Chem. Lett.* **2003**, *32*, 766; b) Y. Nakayama, H. Bando, Y. Sonobe, T. Fujita, *J. Mol. Catal. A: Chem.* **2004**, *213*, 141.
- [4] a) J. Q. Wu, L. Pan, N. H. Hu, Y. S. Li, *Organometallics* **2008**, *27*, 3840; b) J. Q. Wu, L. Pan, S. R. Liu, L. P. He, Y. S. Li, *J. Polym. Sci., Part a: Polym. Chem.* **2009**, *47*, 3573; c) J. Q. Wu, L. Pan, Y. G. Li, S. R. Liu, Y. S. Li, *Organometallics* **2009**, *28*, 1817; d) B. C. Xu, T. Hu, J. Q. Wu, N. H. Hu, Y. S. Li, *Dalton Trans.* **2009**, *41*, 8854; e) J. Q. Wu, B. X. Li, S. W. Zhang, Y. S. Li, *J. Polym. Sci., Part a: Polym. Chem.* **2010**, *48*, 3062; f) J. Q. Wu, Y. G. Li, B. X. Li, Y. S. Li, *Chin. J. Polym. Sci.* **2011**, *29*, 627; g) J. B. Wang, L. P. Lu, J. Y. Liu, H. L. Mu, Y. S. Li, *J. Mol. Catal. A: Chem.* **2015**, *398*, 289.
- [5] a) K. Nomura, A. Sagara, Y. Imanishi, *Chem. Lett.* **2001**, *30*, 36; b) K. Nomura, A. Sagara, Y. Imanishi, *Macromolecules* **2002**, *35*, 1583; c) W. Wang, J. Yamada, M. Fujiki, K. Nomura, *Cat. Com.* **2003**, *4*, 159; d) W. Wang, K. Nomura, *Macromolecules* **2005**, *38*, 5905; e) Y. Onishi, S. Katao, M. Fujiki, K. Nomura, *Organometallics* **2008**, *27*, 2590; f) K. Nomura, A. Igarashi, S. Katao, W. Zhang, W. H. Sun, *Inorg. Chem.* **2013**, *52*, 2607; g) W. Wang, K. Nomura, *Adv. Synth. Catal.* **2006**, *348*, 743; h) A. Igarashi, E. L. Kolychev, M. Tamm, K. Nomura, *Organometallics* **2016**, *35*, 1778; i) K. Nomura, T. Mitsudome, A. Igarashi, G. Nagai, K. Tsutsumi, T. Ina, T. Omiya, H. Takaya, S. Yamazoe, *Organometallics* **2017**, *36*, 530; j) C. Bariashir, C. Huang, G. A. Solan, W.-H. Sun, *Coord. Chem. Rev.* **2019**, *385*, 208.
- [6] a) C. Redshaw, L. Warford, S. H. Dale, M. R. J. Elsegood, *Chem. Commun.* **2004**, 1954; b) C. Redshaw, M. A. Rowan, D. M. Homden, S. H. Dale, M. R. Elsegood, S. Matsui, S. Matsuura, *Chem. Commun.* **2006**, 3329; c) D. M. Homden, C. Redshaw, D. L. Hughes, *Inorg. Chem.* **2007**, *46*, 10827; d) L. Clowes, M. Walton, C. Redshaw, Y. Chao, A. Walton, P. Elo, V. Sumerin, D. L. Hughes, *Cat. Sci. Technol.* **2013**, *3*, 152; e) J. Ma, K. Q. Zhao, M. J. Walton, J. A. Wright, J. W. Frese, M. R. Elsegood, Q. F. Xing, W. H. Sun, C. Redshaw, *Dalton Trans.* **2014**, *43*, 8300; f) J. Ma,

- K. Q. Zhao, M. Walton, J. A. Wright, D. L. Hughes, M. R. Elsegood, K. Michiue, X. Sun, C. Redshaw, *Dalton Trans.* **2014**, *43*, 16698; g) C. Redshaw, M. J. Walton, D. S. Lee, C. Jiang, M. R. Elsegood, K. Michiue, *Chem. A Eur. J.* **2015**, *21*, 5199; h) C. Redshaw, Y. Tang, *Chem. Soc. Rev.* **2012**, *41*, 4484.
- [7] a) D. Reardon, F. Conan, S. Gambarotta, G. Yap, Q. Wang, *J. Am. Chem. Soc.* **1999**, *121*, 9318; b) Z. Janas, L. B. Jerzykiewicz, P. Sobota, R. L. Richards, *Chem. Commun.* **1999**, 1105; c) S. Milione, G. Cavallo, C. Tedesco, A. Grassi, *J. Chem. Soc. Dalton Trans.* **2002**, 1839; d) T. Rüther, K. J. Cavell, N. C. Braussaud, B. W. Skelton, A. H. S. White, *J. Chem. Soc. Dalton Trans.* **2002**, 4684; e) D. S. McGuinness, V. C. Gibson, J. W. Steed, *Organometallics* **2004**, *23*, 6288; f) M. Biazek, K. Czaja, *J. Polym. Sci., Part a: Polym. Chem.* **2008**, *46*, 6940; g) G. Leone, I. Pierro, G. Zanchin, A. Forni, F. Bertini, A. Rapallo, G. Ricci, *J. Mol. Catal. A: Chem.* **2016**, 424, 220; h) N. A. Kolosov, V. A. Tuskaev, S. C. Gagieva, I. V. Fedyanin, V. N. Khrustalev, O. V. Polyakova, B. M. Bulychev, *Eur. Polym. J.* **2017**, *87*, 266.
- [8] H. Makio, H. Terao, A. Iwashita, T. Fujita, *Chem. Rev.* **2011**, *111*, 2363.
- [9] E. Yao, J. Wang, Z. Chen, Y. Ma, *Macromolecules* **2014**, *47*, 8164.
- [10] A. Li, H. Ma, J. Huang, *Appl. Organomet. Chem.* **2013**, *27*, 341. S. Matsui, T. Fujita, *Catal. Today* **2001**, *66*, 63.
- [11] H. Terao, A. Iwashita, N. Matsukawa, S. Ishii, M. Mitani, H. Tanaka, T. Nakano, T. Fujita, *ACS Catal.* **2011**, *1*, 254.
- [12] S. Ay, M. Neiger, S. Bräse, *Chem. A Eur. J.* **2008**, *14*, 11539.
- [13] D. F. Evans, *J. Chem. Soc.* **1959**, 2003.
- [14] aA. Gansnuer, *Tetrahedron* **2002**, *58*, 7017. bA. K. Tomov, V. C. Gibson, D. Zaher, M. R. J. Elsegood, S. H. Dale, *Chem. Commun.* **2004**, 1956.
- [15] A. Gansäuer, B. A. Rinker, *Tetrahedron* **2002**, *58*, 7017.

SUPPORTING INFORMATION

Additional supporting information may be found online in the Supporting Information section at the end of this article.

How to cite this article: Hao Z, Li F, Gao W. *o*-Trityl phenoxy-imino vanadium (III) complexes: synthesis, characterization, and catalysis on ethylene (co)polymerization. *Appl Organomet Chem.* 2020;e5809. <https://doi.org/10.1002/aoc.5809>